Available online at www.sciencedirect.com
ScienceDirect
Journal of Sound and Vibration 310 (2008) 865–880
JOURNAL OF SOUND AND VIBRATION
www.elsevier.com/locate/jsvi

A model for piezo-resistive damping of two-dimensional structures

Oliver M. Fein*

Institute A of Mechanics, Stuttgart University, Pfaffenwaldring 9, 70550 Stuttgart, Germany

Received 15 February 2007; received in revised form 5 August 2007; accepted 8 August 2007
Available online 29 September 2007

Abstract

This work focuses on describing damping enhancement for two-dimensional structures using piezoelectrics in combination with a passive electrical network. An analytical model is developed to quantify such damping. For optimal placement of the piezoelectric elements on a host structure an energy-based approach is applied and extended for two-dimensional structures. Furthermore, the effect of using different configurations of the passive electrical network is discussed. Finally, experiments are conducted to verify the developed models.

1. Introduction

Damping of mechanical vibrations is important because it can reduce the risk of fatigue in materials and reduce structural born sound. Much effort has been expended in attempting to minimize unwanted vibrations. The use of viscoelastic materials with high loss factors is one of the most common damping approaches. One of the drawbacks in using such materials is that they add significant mass to the structure to which they are attached. This is becoming more and more limiting as nowadays light weight structural design is becoming state-of-the-art. Alternatively, piezoelectrics can be used as the primary damping mechanism. They have the unique ability to strain when an electrical voltage is applied and produce an electrical voltage when strained. In short, they have the ability to transform electrical energy to mechanical energy and vice versa. Used in the semi-passive approach the electrical energy is dissipated as heat in a resistor. This approach is regarded as simple, low-cost, light-weight, and easy-to-implement.

First activities in using piezoelectric materials for damping vibrations have been reported in a patent by Forward [1] in 1979. In 1980, Edwards et al. [2] started considerations of theoretical models to describe such a damping phenomenon. However, a first validated model, which has been useful for describing piezo-induced damping, has been published in 1991 by Hagood and Flotow [3]. They did their investigations using a vibrating beam. According to their '*shunted piezo technique*', damping enhancement was achieved through application of piezoelectrics and a passive electrical network (PEN). They attributed the increase in damping

*Corresponding author. Current address: Robert Bosch GmbH, Wernerstr. 51, 70469 Stuttgart, Germany.
E-mail address: oliver.fein@nexgo.de

0022-460X/$ - see front matter © 2007 Elsevier Ltd. All rights reserved.
doi:10.1016/j.jsv.2007.08.005

Nomenclature

$\mathbf{A}$	area of electrode
C	capacitance
d	piezoelectric coefficient
$\mathbf{d}$	piezoelectric coefficient matrix
$\mathbf{D}$	electrical displacement
E	Young's modulus
E'	storage modulus
E''	loss modulus
f	eigenfrequency
I	current
$\mathbf{I}$	identity matrix
j	imaginary unit, $j^2 = -1$
k	electromechanical coupling coefficient
k_p	planar coupling coefficient
l_i	ith dimension of a wafer
$\mathbf{L}$	matrix of dimensions for a wafer
R	resistance
s	mechanical compliance
$\mathbf{s}$	mechanical compliance matrix
t	time
U	voltage
$U_{\mathscr{E}}$	stored electrical energy
U_{eff}	effective strain energy
U_s	maximum stored potential energy
U_{tot}	total potential energy
w	deflection in x_3-direction
W	specific damping work
$\mathbf{x}$	eigenvector
x_i	ith spatial coordinate
$\mathbf{X}$	matrix of eigenvectors
Y	admittance
$\mathbf{Y}$	diagonal admittance matrix
Z	impedance
$\mathbf{Z}$	diagonal impedance matrix
$\bar{Z}$	generalized impedance, $\bar{Z} = C^{\sigma} Z^{\text{sp}} j\omega$
η	loss factor
$\boldsymbol{\eta}$	matrix of loss factors
ε	mechanical strain
$\tilde{\varepsilon}$	electrical permittivity
λ	eigenvalue
ν	Poisson's ratio
ω	circular frequency
ρ	dimensionless circular frequency, $\rho = RC^{\mathscr{E}}\omega$
σ	stress
ξ	structural damping
$\mathscr{L}$	inductance
$\mathscr{E}$	electrical field
$(\breve{\cdot})$	quantity in system of principle axes
$(\cdot)_p$	material property of piezoelectric wafer
$(\cdot)^{\text{PEN}}$	quantity of passive electrical network
$(\cdot)^{\text{sp}}$	quantity in semi-passive case
$(\cdot)^{\text{T}}$	transposition of a matrix
$(\cdot)^{\varepsilon}$	quantity for constant mechanical strain
$(\cdot)^{\sigma}$	quantity for constant mechanical stress
$(\cdot)^{\mathscr{E}}$	quantity for constant electrical field

basically to two features: (1) the type of PEN they used and (2) the electromechanical coupling coefficient of the piezoelectric material. For their investigations they used resistors and a combination of resistor and inductor (RL). They observed an increase in damping over a broad frequency regime by using a resistive PEN. The damping could be significantly increased by using a RL-combination. However, the frequency range was limited, and additionally, a rather large inductor of 142.4 H was required for optimal damping. Publications of others [4–7] conclude with similar results concerning the high inductances for optimal damping treatment. From a practical point of view this high inductance limits the application of a RL-combination significantly. Park et al. [8] worked on an improved PEN composed of a capacitor C in parallel with the RL-combination. As a consequence of the capacitor, the optimal inductance is reduced by $1/(1+\alpha)$, where α is the ratio of the capacitance C to the capacitance of the piezoelectric element used.

A stack actuator utilizing the shunted piezo technique is modeled by Law et al. [9]. Moreover they stress that Hagood's [3] model is limited to frequencies well below the first eigenfrequency of the piezoelectric element.

Based on the results in Ref. [3] Davis et al. [10] formulated the '*effective strain energy*' for uniaxial stress for a slender beam-like piezoelectric element. The ratio of effective strain energy to total maximum strain energy, which is stored in a vibrating structure, allows the prediction of increased damping for each single mode of the beam. This concept can be applied for arbitrary positions of the piezoelectric element with respect to the base structure. Conducting experiments with different positions of piezoelectric elements on a beam verified this method.

A good survey of historical and recent research activities on damping enhancement by using piezoelectric materials is given in Refs. [4,5]. There are also some publications about the shunted piezo technique applied to plate-like structures [11–13]. However, these investigations present no analytical expression for the damping enhancement due to the chosen damping treatment.

This work primarily extends the existing models which are all restricted to one-dimensional structures to the two-dimensional case. Plate-like structures are widely used in practice, and they are also most interesting from a sound emission point of view. Based on matrix operations and analytical formulations, for the first time, an analytical model for two-dimensional structures is presented. Compared to models proposed in literature so far this model can be used to precisely predict the increase in damping of vibrating plates. Material properties of the piezoelectric elements and the properties of the passive electrical network are identified as most important parameters. Furthermore, the effective strain energy approach is derived for two-dimensional structures. So far it is only existing for simple one-dimensional beams. It is also shown that the one-dimensional case is incorporated in the more general two-dimensional formulation. Such a two-dimensional formulation is crucial for optimizing the layout of the piezoelectric elements which are applied on the structure under investigation. Finally, the models are verified by a series of experiments conducted on a vibrating plate.

2. A model of piezo-resistive damping

Typically, the piezoelectric effect is described by using the mechanical stress $\boldsymbol{\sigma}$ and the electrical field $\boldsymbol{\mathscr{E}}$ vectors as independent state variables. Thus the set of linear equations is of the $(\sigma, \mathscr{E})$-type, as outlined by Ikeda [14]. The mechanical strain $\boldsymbol{\varepsilon}$ and electrical displacement $\mathbf{D}$ are given by

$$\begin{bmatrix} \varepsilon \\ \mathbf{D} \end{bmatrix} = \begin{bmatrix} \mathbf{s}^{\mathscr{E}} & \mathbf{d}^{\mathrm{T}} \\ \mathbf{d} & \tilde{\varepsilon}^{\sigma} \end{bmatrix} \begin{bmatrix} \sigma \\ \mathscr{E} \end{bmatrix}. \tag{1}$$

In this representation $\mathbf{s}^{\mathscr{E}}$ denotes the mechanical compliance matrix for constant electrical field, $\mathbf{d}$ is the piezoelectric coefficient matrix, and $\tilde{\boldsymbol{\varepsilon}}^{\sigma}$ is the electrical permittivity matrix for constant stress. The index T denotes the transposition of a matrix. An electrical field and electrical displacement give rise to an electrical voltage and current, respectively. These quantities can be calculated as

$$\mathbf{U} = \int (\mathscr{E}_1 \,\mathrm{d}x_1 + \mathscr{E}_2 \,\mathrm{d}x_2 + \mathscr{E}_3 \,\mathrm{d}x_3) \tag{2}$$

$$I_i = \frac{\mathrm{d}}{\mathrm{d}t} Q_i = \int_{A_i} \frac{\mathrm{d}}{\mathrm{d}t} \tilde{D}_i \,\mathrm{d}a_i. \tag{3}$$

Both quantities are dependent on time and the spatial coordinates, where the time dependency can be expressed as $\tilde{D}_i = D_i \mathrm{e}^{\mathrm{j}\omega t}$. This yields the representation

$$\mathbf{U} = \mathbf{L}\mathscr{E}, \quad \mathbf{I} = \mathbf{A}\mathrm{j}\omega\mathbf{D}, \tag{4}$$

where the electric field and electric displacement are assumed constant, and $\mathrm{j}^2 = -1$. The matrix $\mathbf{L} = \mathrm{diag}\{\ell_i\}$ characterizes the dimensions of a piezoelectric wafer, as shown in Fig. 1(a). Using Eqs. (1) and (4)

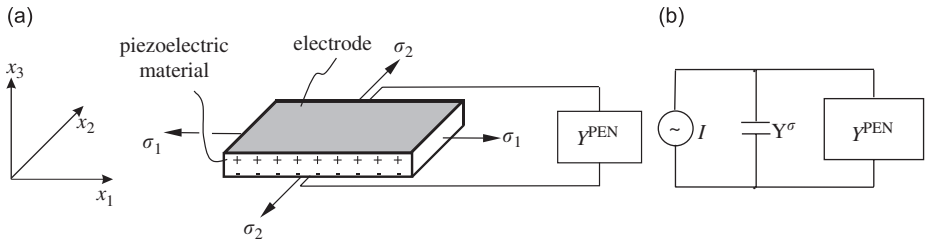

Fig. 1. Models of semi-passive piezoelectric elements: (a) semi-passive piezo-wafer and (b) electrical model [9].

a formulation relating strain and current to stress and voltage is derived,

$$\begin{bmatrix} \varepsilon \\ \mathbf{I} \end{bmatrix} = \begin{bmatrix} \mathbf{s}^{\mathscr{E}} & \mathbf{d}^{\mathrm{T}}\mathbf{L}^{-1} \\ \mathrm{j}\,\omega\mathbf{A}\,\mathbf{d} & \mathrm{j}\omega\mathbf{A}\tilde{\varepsilon}^{\sigma}\mathbf{L}^{-1} \end{bmatrix} \begin{bmatrix} \sigma \\ \mathbf{U} \end{bmatrix} \tag{5}$$

$$= \begin{bmatrix} \mathbf{s}^{\mathscr{E}} & \mathbf{d}^{\mathrm{T}}\mathbf{L}^{-1} \\ \mathrm{j}\omega\mathbf{A}\,\mathbf{d} & \mathbf{Y}^{\sigma} \end{bmatrix} \begin{bmatrix} \sigma \\ \mathbf{U} \end{bmatrix}. \tag{6}$$

For simplification of Eq. (6) the relationship for a plate capacitor

$$C_i^{\sigma} = A_i\tilde{\varepsilon}_{ii}^{\sigma}/\ell_i \tag{7}$$

is used which is valid for constant stress. Furthermore, the admittance Y^{σ} for a piezoelectric wafer under constant mechanical stress is given as $Y^{\sigma} = \mathrm{j}\,\omega C^{\sigma}$. Applying a PEN to the piezo-wafer results in energy dissipation and, thus, in an enhancement of damping. Fig. 1 shows a PEN in parallel with a piezo-wafer as well as the resulting equivalent circuit diagram, known as the Thevenin-equivalent circuit diagram. This equivalent circuit diagram is only valid for a piezo-wafer which is working well below its first eigenfrequency (quasi-static case). It has been introduced by Law et al. [9]. It is possible to apply three independent PENs, each acting in one spatial direction within the piezo-wafer. Consequently, the matrix of admittance for all PENs shows merely diagonal entries, $\mathbf{Y}^{\mathrm{PEN}} = \mathrm{diag}\{Y_i^{\mathrm{PEN}}\}$. For admittances working in parallel, the total admittance is given by the sum of all single admittances [15]. Therefore, a shunted piezoelectric element can be characterized as

$$\begin{bmatrix} \varepsilon \\ \mathbf{I} \end{bmatrix} = \begin{bmatrix} \mathbf{s}^{\mathscr{E}} & \mathbf{d}^{\mathrm{T}}\mathbf{L}^{-1} \\ \mathrm{j}\omega\mathbf{A}\,\mathbf{d} & \mathbf{Y}^{\mathrm{sp}} \end{bmatrix} \begin{bmatrix} \sigma \\ \mathbf{U} \end{bmatrix} \quad \text{with } \mathbf{Y}^{\mathrm{sp}} = \mathbf{Y}^{\sigma} + \mathbf{Y}^{\mathrm{PEN}}, \tag{8}$$

where the index sp denotes the shunted case. The electrical voltage of a shunted piezoelectric element is given by

$$\mathbf{U} = \mathbf{Z}^{\mathrm{sp}}(\mathbf{I} - \mathrm{j}\omega\mathbf{A}\,\mathbf{d}\sigma). \tag{9}$$

The impedance matrix $\mathbf{Z}^{\mathrm{sp}}$ is also diagonal and results from an inversion of the admittance, $\mathbf{Z}^{\mathrm{sp}} = (\mathbf{Y}^{\mathrm{sp}})^{-1}$. The voltage $\mathbf{U}$ in Eq. (8) can be eliminated by using Eq. (9). This yields a linear relation for the strain in a shunted piezo-wafer

$$\varepsilon = (\mathbf{s}^{\mathscr{E}} - \mathrm{j}\omega\,\mathbf{d}^{\mathrm{T}}\mathbf{L}^{-1}\mathbf{Z}^{\mathrm{sp}}\mathbf{A}\,\mathbf{d})\sigma + \mathbf{d}^{\mathrm{T}}\mathbf{L}^{-1}\mathbf{Z}^{\mathrm{sp}}\mathbf{I}. \tag{10}$$

For the following considerations the applied current is set to zero. This means the piezoelectric element is not actively driven. The compliance matrix of a purely shunted piezo-wafer can be written as

$$\mathbf{s}^{\mathrm{sp}} = \mathbf{s}^{\mathscr{E}} - \mathrm{j}\omega\,\mathbf{d}^{\mathrm{T}}\mathbf{L}^{-1}\mathbf{Z}^{\mathrm{sp}}\mathbf{A}\,\mathbf{d}. \tag{11}$$

Taking into account the definition of a plate capacitor, Eq. (7), yields

$$\begin{aligned} \mathbf{s}^{\mathrm{sp}} &= \mathbf{s}^{\mathscr{E}} - \mathrm{j}\omega\,\mathbf{d}^{\mathrm{T}}\mathbf{C}^{\sigma}\tilde{\varepsilon}^{\sigma^{-1}}\mathbf{Z}^{\mathrm{sp}}\mathbf{d} \\ &= \mathbf{s}^{\mathscr{E}} - \mathbf{d}^{\mathrm{T}}\bar{\mathbf{Z}}^{\mathrm{sp}}\tilde{\varepsilon}^{\sigma^{-1}}\mathbf{d} \quad \text{with} \quad \bar{\mathbf{Z}}^{\mathrm{sp}} = \mathbf{C}^{\sigma}\mathbf{Z}^{\mathrm{sp}}\mathrm{j}\omega \end{aligned} \tag{12}$$

for the compliance of a shunted piezo-wafer, where the generalized impedance $\bar{\mathbf{Z}}^{\mathrm{sp}}$ is introduced. The matrices $\bar{\mathbf{Z}}^{\mathrm{sp}}$ and $\tilde{\boldsymbol{\varepsilon}}^{\sigma^{-1}}$ are diagonal matrices. Thus, the following relationship holds:

$$\mathbf{d}^{\mathrm{T}}\bar{\mathbf{Z}}^{\mathrm{sp}}\tilde{\varepsilon}^{\sigma^{-1}}\mathbf{d} = \mathbf{d}^{\mathrm{T}}\,\mathrm{diag}\{\bar{Z}^{\mathrm{sp}}/\tilde{\varepsilon}^{\sigma}\}\,\mathbf{d} = \sum_{i=1}^{3}(\bar{Z}_{ii}^{\mathrm{sp}}/\tilde{\varepsilon}_{ii}^{\sigma})\,\mathbf{d}_i^{\mathrm{T}}\,\mathbf{d}_i, \tag{13}$$

where $\mathbf{d}_i$ characterizes the ith row of the matrix $\mathbf{d}$. The subscripts ii denote the diagonal element of the corresponding matrix. Substituting Eq. (13) into Eq. (12), one obtains

$$\mathbf{s}^{\mathrm{sp}} = \mathbf{s}^{\mathscr{E}} - \sum_{i=1}^{3} (\bar{Z}_{ii}^{\mathrm{sp}} / \tilde{\varepsilon}_{ii}^{\sigma})\, \mathbf{d}_i^{\mathrm{T}}\, \mathbf{d}_i = \mathbf{s}^{\mathscr{E}} - \sum_{i=1}^{3} (\bar{Z}_{ii}^{\mathrm{sp}} / \tilde{\varepsilon}_{ii}^{\sigma})\, \mathbf{M}_i. \tag{14}$$

The elements of the resulting matrix $\mathbf{M}_i$ are proportional with respect to the piezo-electric coefficients of the piezo-electric material and can be computed as

$$\mathbf{M}_1 = \begin{bmatrix} 0 & 0 & 0 & 0 & 0 & 0 \\ 0 & 0 & 0 & 0 & 0 & 0 \\ 0 & 0 & 0 & 0 & 0 & 0 \\ 0 & 0 & 0 & 0 & 0 & 0 \\ 0 & 0 & 0 & 0 & d_{15}^2 & 0 \\ 0 & 0 & 0 & 0 & 0 & 0 \end{bmatrix}, \quad \mathbf{M}_2 = \begin{bmatrix} 0 & 0 & 0 & 0 & 0 & 0 \\ 0 & 0 & 0 & 0 & 0 & 0 \\ 0 & 0 & 0 & 0 & 0 & 0 \\ 0 & 0 & 0 & d_{15}^2 & 0 & 0 \\ 0 & 0 & 0 & 0 & 0 & 0 \\ 0 & 0 & 0 & 0 & 0 & 0 \end{bmatrix},$$

$$\mathbf{M}_3 = \begin{bmatrix} d_{31}^2 & d_{31}^2 & d_{31}d_{33} & 0 & 0 & 0 \\ d_{31}^2 & d_{31}^2 & d_{31}d_{33} & 0 & 0 & 0 \\ d_{31}d_{33} & d_{31}d_{33} & d_{33}^2 & 0 & 0 & 0 \\ 0 & 0 & 0 & 0 & 0 & 0 \\ 0 & 0 & 0 & 0 & 0 & 0 \\ 0 & 0 & 0 & 0 & 0 & 0 \end{bmatrix}. \tag{15}$$

In cases where the electrodes of the piezo-wafer are applied within the x_2x_3- or x_1x_3-plane, the compliance is only dependent on d_{15}, as can be seen for matrix $\mathbf{M}_1$ and $\mathbf{M}_2$. However, if the electrodes are applied within the x_1x_2-plane, the resulting compliance is dependent on d_{31} as well as d_{33}. This configuration is of special interest for the case of piezo-wafers which are used in the 31-mode, i.e., wafers which are polarized in the x_3-direction and stressed in the x_1-direction (see Fig. 1(a)).

2.1. Passive electrical network

The introduced PEN can be realized in three different ways: (1) Using a capacitance C, which results in a capacitive PEN (2) by the use of an inductance $\mathscr{L}$, which is termed an inductive PEN or (3) alternatively, by a resistance R, the so-called resistive PEN. All three possibilities are illustrated in Fig. 2.

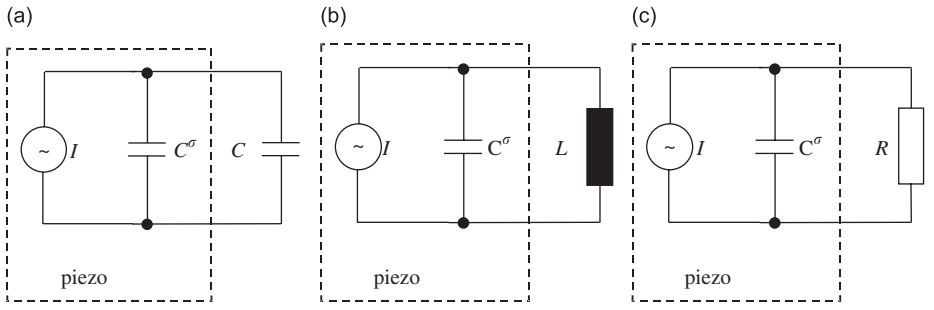

Fig. 2. Different techniques to realize a shunted piezo: (a) capacitive, (b) inductive and (c) resistive.

The application of a capacitive PEN yields the generalized impedance:

$$\bar{Z}^{\mathrm{sp}} = \frac{C^{\sigma}}{C + C^{\sigma}}, \tag{16}$$

whereby the total admittance is expressed by means of Eq. (8) with $Y^{\mathrm{PEN}} = C\mathrm{j}\omega$ and $Y^{\sigma} = C^{\sigma}\mathrm{j}\omega$. This configuration only changes the compliance of the shunted piezo-wafer. No damping increase is observed for this configuration [3,4].

For an inductor in parallel with the piezo-wafer, the admittance of the piezoelectric element and the inductor can be written as $Y^{\sigma} = C^{\sigma}\mathrm{j}\omega$ and $Y^{\mathrm{PEN}} = 1/\mathscr{L}\mathrm{j}\omega$, respectively. Finally, for the generalized impedance one finds

$$\bar{Z}^{\mathrm{sp}} = \frac{C^{\sigma}\mathscr{L}\omega^2}{C^{\sigma}\mathscr{L}\omega^2 - 1}. \tag{17}$$

A suitable choice of the inductance results in a reduction in vibration, as has been shown by Hagood and von Flotow [3] for a slender beam-like piezoelectric element. However, a significant increase in damping is only given in a very narrow frequency range. For other frequencies or for a detuned inductor the vibration reduction is negligible [3,5,7]. Additionally, the very high values for the inductance of approximately 100 H for frequencies below 1 kHz are very restrictive from a practical point of view [3–7].

The technical realization of a resistive PEN is relatively simple, because a resistor is very small in weight and size. Within the resistor some part of the vibration energy is dissipated as heat. This results in a very good vibration reduction [3,4,16–18]. In Ref. [19] a method is presented which describes how the resistance can be automatically adapted over a broad frequency regime. A phase shift of $-\pi/2$ for the voltage has to be taken into account when R is in parallel with C^{σ}. Furthermore, the admittance of the piezo and the PEN are given by $Y^{\sigma} = C^{\sigma}\mathrm{j}\omega$ and $Y^{\mathrm{PEN}} = 1/R$, respectively, which yields

$$\bar{Z}^{\mathrm{sp}} = \frac{RC^{\sigma}\mathrm{j}\,\omega}{RC^{\sigma}\mathrm{j}\omega + 1} \tag{18}$$

for the generalized impedance. The capacitance C^{σ} of the piezoelectric element in Eqs. (16), (17), and (18) is only valid for constant stress conditions within a piezo-wafer. However, for a piezo-wafer applied to a structure, the mechanical strain within this element is constant. This effects the capacitance of the piezoelectric element. According to Ikeda [14] this change in capacitance is found to be

$$C^{\varepsilon} = C^{\sigma}(1 - k^2), \tag{19}$$

where the electromechanical coupling coefficient k is introduced. The parameter k is dependent on how the stresses are applied [14]. The generalized impedance for a resistively shunted piezo-wafer under constant mechanical strain can be written as

$$\bar{Z}^{\mathrm{sp}} = \frac{\mathrm{j}}{\mathrm{j}\rho + 1 - k^2} \qquad \text{with } \rho = RC^{\varepsilon}\omega, \tag{20}$$

where ρ denotes the dimensionless circular frequency.

2.2. Damping effect of a two-dimensional piezo-wafer

For damping treatment of thin-walled vibrating structures, the 31-mode of a shunted piezo is of particular interest. The piezoelectric wafer is therefore bonded on a vibrating structure. The piezoelectric element is polarized in the x_3-direction, and a resistive PEN is connected to the x_1x_2-electrodes. Within the piezo-wafer a plane-stress field with $\sigma_3 = \sigma_4 = \sigma_5 = 0$ is effective. Based on Eq. (14) and assuming transversal-isotropic properties for the piezoelectric material yields the compliance for a resistively shunted piezo-wafer with

Poisson's ratio v

$$\mathbf{s}^{\mathrm{sp}} = \begin{bmatrix} s_{11}^{\mathscr{E}} & -vs_{11}^{\mathscr{E}} & 0 \\ -vs_{11}^{\mathscr{E}} & s_{11}^{\mathscr{E}} & 0 \\ 0 & 0 & 2(1+v)s_{11}^{\mathscr{E}} \end{bmatrix} - \frac{\bar{Z}_{33}^{\mathrm{sp}}}{\tilde{\varepsilon}_{33}^{\sigma_p}} \begin{bmatrix} d_{31}^2 & d_{31}^2 & 0 \\ d_{31}^2 & d_{31}^2 & 0 \\ 0 & 0 & 0 \end{bmatrix}. \tag{21}$$

According to Ikeda [14] it is necessary to introduce the electrical permittivity $\tilde{\varepsilon}_{33}^{\sigma_p}$, due to plane-stress conditions. It has to be added that $\tilde{\varepsilon}_{33}^{\sigma}$ is only valid for the uniaxial stress condition. Additionally, it is taken into account that $\bar{Z}^{\mathrm{sp}}$ for a resistive PEN obeys Eq. (20) which finally yields

$$\mathbf{s}^{\mathrm{sp}} = \begin{bmatrix} s_{11}^{\mathscr{E}} & -vs_{11}^{\mathscr{E}} & 0 \\ -vs_{11}^{\mathscr{E}} & s_{11}^{\mathscr{E}} & 0 \\ 0 & 0 & 2(1+v)s_{11}^{\mathscr{E}} \end{bmatrix} - \frac{m\rho(\rho + (1-k_p^2)\mathrm{j})}{(1-k_p^2)^2 + \rho^2} \begin{bmatrix} 1 & 1 & 0 \\ 1 & 1 & 0 \\ 0 & 0 & 0 \end{bmatrix}, \tag{22}$$

where the constant

$$m = d_{31}^2(1-k_p^2)/\tilde{\varepsilon}_{33}^{\sigma} \tag{23}$$

is introduced. The constant $(1-k_p^2)$ in Eq. (23) is used to scale the electrical permittivity $\tilde{\varepsilon}^{\sigma}$, as required by the plane-stress condition [14,20]. For an isotropic piezoelectric material under plane-stress conditions, the planar coupling coefficient k_p is given by Ikeda [14]

$$k_p = \sqrt{\frac{2d_{31}^2}{\tilde{\varepsilon}_{33}^{\sigma} s_{11}(1-v)}}. \tag{24}$$

2.2.1. Damping under plane-stress conditions

It can be shown, that the complex matrix $\mathbf{s}^{\mathrm{sp}}$ in Eq. (22) is normal, $\mathbf{A}\mathbf{A}^* = \mathbf{A}^*\mathbf{A}$, where $\mathbf{A}^*$ is the conjugate of $\mathbf{A}$. Hence, there exists a complete set of orthogonal eigenvectors, and the matrix can be diagonalized [21].

The characteristic polynomial of $\mathbf{s}^{\mathrm{sp}}$ is of third order. The resulting roots are the eigenvalues of $\mathbf{s}^{\mathrm{sp}}$,

$$\lambda_1 = \frac{2\rho m + s_{11}^{\mathscr{E}}(v-1)(\rho + \mathrm{j}(k_p^2-1))}{\rho^2 + (k_p^2-1)^2}(-\rho + \mathrm{j}(k_p^2-1)), \tag{25}$$

$$\lambda_2 = (1+v)s_{11}^{\mathscr{E}}, \tag{26}$$

$$\lambda_3 = 2(1+v)s_{11}^{\mathscr{E}}. \tag{27}$$

In the case of λ_1, which is complex in nature, the rank of $(\mathbf{s}^{\mathrm{sp}} - \lambda_1\mathbf{I})$ is found to be two. The corresponding eigenvector is given as

$$\mathbf{x}_1^{\mathrm{T}} = 1/\sqrt{2}(1,1,0)^{\mathrm{T}}. \tag{28}$$

It is normalized such that its Euclidean norm is unity. For the other two eigenvalues λ_2 and λ_3, the linearly independent and normalized eigenvectors are computed to be

$$\mathbf{x}_2^{\mathrm{T}} = 1/\sqrt{2}(-1,1,0)^{\mathrm{T}}, \tag{29}$$

$$\mathbf{x}_3^{\mathrm{T}} = (0,0,1)^{\mathrm{T}}. \tag{30}$$

The three eigenvectors can be arranged into the matrix of eigenvectors $\mathbf{X} = [\mathbf{x}_1, \mathbf{x}_2, \mathbf{x}_3]$ such that

$$\mathbf{X}^{-1}\mathbf{s}^{\mathrm{sp}}\mathbf{X} = \check{\mathbf{s}}^{\mathrm{sp}} \tag{31}$$

where $\check{\mathbf{s}}^{\mathrm{sp}}$ is a diagonal matrix whose entries correspond to the eigenvalues. The operation $(\check{\cdot})$ denotes transformation to the principal axes.

Following investigations done by Hagood [3] for the one-dimensional loading case of a shunted piezo, the complex Young's modulus is introduced. It is defined in the frequency domain as

$$\underline{E}(\omega) = E'(\omega) + \mathrm{j}E''(\omega), \tag{32}$$

where the real and imaginary parts are referred to as the storage and loss modulus, respectively. Introducing the loss factor η, the complex modulus can be written as

$$\underline{E}(\omega) = E'(\omega)[1 + \mathrm{j}\eta(\omega)], \tag{33}$$

$$\eta(\omega) = \frac{E''(\omega)}{E'(\omega)} = \frac{\mathrm{Im}(\underline{E}(\omega))}{\mathrm{Re}(\underline{E}(\omega))}. \tag{34}$$

According to the relationship $\mathbf{E} = \mathbf{s}^{-1}$ the stiffness matrix $\check{\mathbf{E}}^{\mathrm{sp}}$ for a shunted piezo-wafer is given by

$$\check{\mathbf{E}}^{\mathrm{sp}} = \begin{bmatrix} 1/\lambda_1 & 0 & 0 \\ 0 & 1/\lambda_2 & 0 \\ 0 & 0 & 1/\lambda_3 \end{bmatrix}. \tag{35}$$

After splitting the coefficients in Eq. (35) into their real and imaginary parts and applying Eq. (34) the loss factors result

$$\check{\eta}_1 = \frac{2\rho m(k_p^2 - 1)}{2\rho^2 m + s_{11}^{\mathscr{E}}(\nu - 1)[\rho^2 + (k_p^2 - 1)^2]},$$
$$\check{\eta}_2 = \check{\eta}_3 = 0. \tag{36}$$

Finally, the loss factors, which are expressed in terms of the principal axes have to be re-transformed according to

$$\boldsymbol{\eta} = \mathbf{X}\check{\boldsymbol{\eta}}\mathbf{X}^{-1}. \tag{37}$$

This results in the matrix of loss factors

$$\boldsymbol{\eta} = \frac{\rho m(k_p^2 - 1)}{2\rho^2 m + s_{11}^{\mathscr{E}}(\nu - 1)[\rho^2 + (k_p^2 - 1)^2]} \begin{bmatrix} 1 & 1 & 0 \\ 1 & 1 & 0 \\ 0 & 0 & 0 \end{bmatrix}. \tag{38}$$

Taking into account the definition of the parameter m, Eq. (23), and the planar coupling coefficient k_p, Eq. (24), a scalar loss factor may be defined as

$$\eta = \frac{\rho k_p^2 (k_p^2 - 1)^2}{2(\rho^2 k_p^2 (k_p^2 - 1) + \rho^2 + (k_p^2 - 1)^2)}. \tag{39}$$

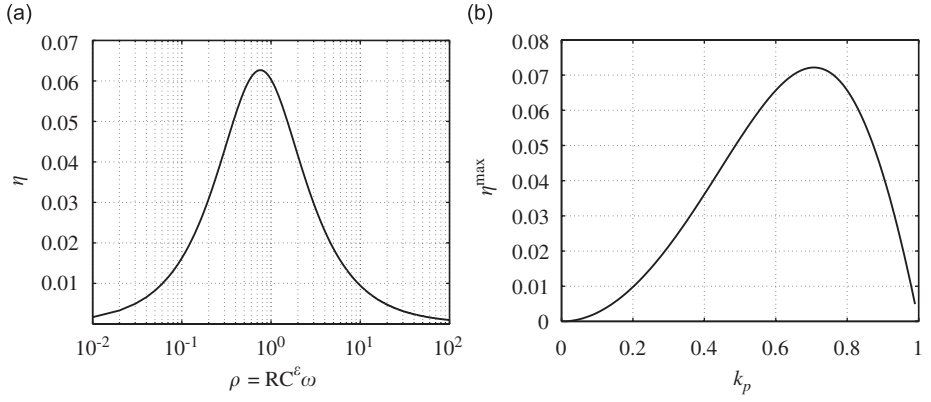

Fig. 3. Piezo-resistive damping for two-dimensional loading: (a) loss factor η (for $k_p = 0.58$) vs. ρ and (b) maximum loss factor $\eta^{\max}$ vs. planar coupling coefficient k_p.

Fig. 3(a) illustrates the relationship between loss factor η and dimensionless frequency ρ for a resistively shunted piezo-wafer with a typical coupling coefficient $k_p = 0.58$ [22]. It clearly shows a maximum loss factor $\eta^{\max}$ which can be calculated as

$$\eta^{\max} = \frac{1}{4} k_p^2 \sqrt{\frac{(k_p-1)^2(k_p+1)^2}{k_p^4 - k_p^2 + 1}}, \tag{40}$$

$$\text{at} \quad \rho_{\eta\text{-max}} = \frac{(k_p+1)(1-k_p)}{\sqrt{k_p^4 - k_p^2 + 1}} = RC^{\mathscr{E}}\omega. \tag{41}$$

According to Eq. (41), the maximum loss factor can be shifted to any frequency by adjusting the PEN's resistance R. This is based on the fact, that the capacitance of the piezo-wafer is constant as long as it is driven below its first mechanical eigenfrequency [14,17]. Eq. (40) clearly indicates that the maximum loss factor is only dependent on k_p. The maximum loss factor $\eta^{\max}$ is plotted as a function of the planar coupling coefficient k_p in Fig. 3. Typical values for k_p range from 0.04 for polyvinylidene–fluoride–films (PVDF) [23] to 0.62 for lead–zirconate–titanate (PZT) [22]. Such a comparison shows, that it is advantageous to use PZT for piezo-resistive damping in order to reach high loss factors.

3. Piezo-resistive damping for plates

To reduce vibrations of a structure, viscoelastic elements can be applied to it. The loss factor of one such element is characterized as [24]

$$\eta_i = \frac{W_{s_i}}{2\pi\, U_{s_i}}. \tag{42}$$

In this representation, η_i is proportional to the ratio of the specific damping work W_{s_i} to a reference energy. For a linear viscoelastic material this reference energy equals the maximum stored potential energy U_{s_i} of the ith damping element. If several such elements are attached to a structure, the resulting loss factor for the entire structure (plate and viscoelastic elements) is given as

$$\eta = \frac{\sum W_{s_i}}{2\pi U_{\text{tot}}} = \frac{\sum \eta_i\, U_{s_i}}{U_{\text{tot}}}. \tag{43}$$

The loss factor of such a layered structure is proportional to the ratio of dissipated energy to total potential energy of the layered structure. The specific damping work W_{s_i} due to one viscoelastic element is given by means of Eq. (42). Thus, the total loss factor can be expressed as shown in Eq. (43).

The considerations mentioned above are only valid when viscoelasticity is an inherent property of the material. However, for a piezoelectric element the viscoelastic property results from the interaction of the piezoelectric effect with a connected resistive PEN. The energy dissipated in the PEN is proportional to the electrical energy stored within the piezoelectric material. It can be shown, that the stored electrical energy is proportional to the strain energy. For that reason the term *effective strain energy* can be found in the literature [4,10]. The calculation of this energy is shown in the following section. The resulting loss factor for the ith shunted piezo-wafer can be expressed in terms of dissipated energy and the effective strain energy U_{eff_i}, using a relation similar to Eq. (42),

$$\eta_i = W_{s_i}/(2\pi U_{\text{eff}_i}). \tag{44}$$

For N shunted piezo-wafers attached on a structure, the total loss factor for the layered structure is given as

$$\eta = \frac{\sum_{i=1}^{N} \eta_i\, U_{\text{eff}_i}}{U_{\text{tot}}}, \tag{45}$$

where the denominator denotes the total maximum potential energy of the layered structure.

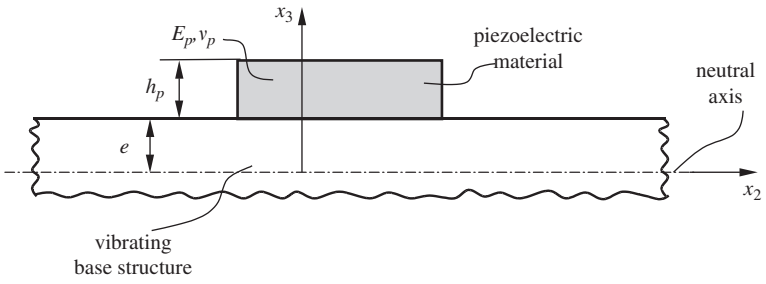

Fig. 4. Plate-like structure with attached piezo-wafer.

3.1. Modified strain energy for a two-dimensional piezo-wafer

The effective strain energy is based on considerations of the electrical energy resulting from the piezoelectric effect. Electrical energy is stored within the piezoelectric element, where the electrical field is effective. The specific electrical energy is defined as [25]

$$\frac{\mathrm{d}U_{\mathscr{E}}}{\mathrm{d}V} = \frac{1}{2}\frac{\mathrm{d}Q_3}{\mathrm{d}A_3}\mathscr{E}_3. \tag{46}$$

In this equation $\mathrm{d}Q_3/\mathrm{d}A_3$ and $\mathscr{E}_3$ denote the electrical displacement and electrical field in the x_3-direction, respectively. The electrical displacement as a result of applied stresses is found using Eq. (1) to be

$$\frac{\mathrm{d}Q_3}{\mathrm{d}A_3} = D_3 = d_{31}(\sigma_1 + \sigma_2) + d_{33}\sigma_3. \tag{47}$$

Consider now a transversely vibrating plate-like structure with bonded piezo-wafers on it, as depicted in Fig. 4. The distance from the neutral axis to the plate's surface is characterized by e. This results in a plane-stress field with $\sigma_3 = 0$ and the classical plate theory holds

$$\sigma_1 = -\frac{E_\mathrm{p} x_3}{1-\nu_\mathrm{p}}(w_{,11} + \nu_\mathrm{p} w_{,22}), \tag{48}$$

$$\sigma_2 = -\frac{E_\mathrm{p} x_3}{1-\nu_\mathrm{p}}(w_{,22} + \nu_\mathrm{p} w_{,11}). \tag{49}$$

In this representation w denotes the deflection in the x_3-direction and $(\cdot)_{,11}$ and $(\cdot)_{,22}$ denote the second spatial derivative with respect to the x_1- and x_2-direction. Taking into account Eqs. (47)–(49) yields

$$\begin{aligned}\frac{\mathrm{d}U_{\mathscr{E}}}{\mathrm{d}V} &= \frac{1}{2\tilde{\varepsilon}_{33}} D_3^2 \\ &= \frac{d_{31}^2}{2\tilde{\varepsilon}_{33}} \frac{E_\mathrm{p}^2 x_3^2 (1+\nu_\mathrm{p})^2}{(1-\nu_\mathrm{p})^2}(w_{,11} + w_{,22})^2 \\ &= k_p^2 x_3^2 \frac{E_\mathrm{p}(1+\nu_\mathrm{p})^2}{4(1-\nu_\mathrm{p})}(w_{,11} + w_{,22})^2,\end{aligned} \tag{50}$$

for the specific electrical energy where the definition of the planar coupling coefficient, Eq. (24), is used. Finally, integration yields

$$U_{\mathscr{E}} = k_p^2 \frac{E_\mathrm{p}(1+\nu_\mathrm{p})^2}{12(1-\nu_\mathrm{p})}[x_3^3]_e^{e+h_\mathrm{p}} \iint_A (w_{,11}^2 + 2w_{,11}w_{,22} + w_{,22}^2)\,\mathrm{d}x_2\,\mathrm{d}x_1, \tag{51}$$

for the stored electrical energy within a rectangular piezo-wafer. It has to be emphasized that this formulation is based on the assumption that the electric flux lines all point in the same direction. However, this is only true when the strain distribution within the wafer is strictly negative or positive. Consider now the case where the piezo-wafer is attached symmetrically to a nodal line. This results in negative strain in one part of the wafer

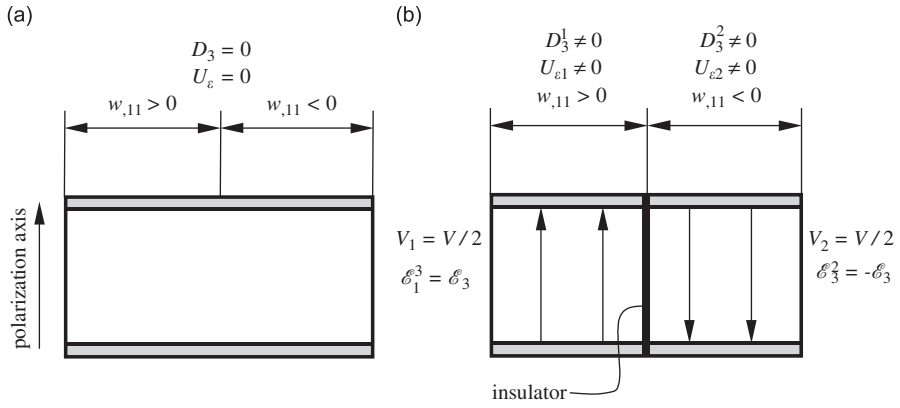

Fig. 5. Electric field within a piezo-wafer: (a) physical situation and (b) model.

and positive strain in the other, as depicted in Fig. 5(a). The net generated electrical charge and therefore stored electrical energy are as a consequence reduced to zero. This is a direct consequence of the piezoelectric effect, which is polar in nature. Applying Eq. (51) in such a case results, however, in a non-zero energy, which can not be explained physically. For this reason, in a thought experiment, an electrical insulating layer is inserted into the piezo-wafer in such a way that it is perpendicular to the electrodes. As a consequence, two electrical fields will be generated, as seen in Fig. 5(b). These fields have the same magnitude, but the phase is shifted by 180°. The total stored energy is now the sum of both energies $U_{\mathscr{E}1}$ and $U_{\mathscr{E}2}$. According to Eq. (46) this energy is given as

$$U_{\mathscr{E}} = \int_{V_1} \frac{1}{2}\frac{\mathrm{d}Q_3}{\mathrm{d}A_3}\mathscr{E}_3\,\mathrm{d}V + \int_{V_2} \frac{1}{2}\frac{\mathrm{d}Q_3}{\mathrm{d}A_3}(-\mathscr{E}_3)\,\mathrm{d}V = 0, \tag{52}$$

where the polar nature of the piezoelectric effect is incorporated. Obviously, the direction of the electrical field is a result of the sign of the strain. This effect is lost in Eq. (51), due to squaring of the curvature terms. However, Eq. (51) can be modified such, that the quadratic terms are replaced by the product of the curvature and the absolute value of the curvature. This results in the effective strain energy for a two-dimensional piezo-wafer

$$U_{\mathrm{eff}} = k_p^2 \frac{E_\mathrm{p}(1+\nu_\mathrm{p})^2}{12(1-\nu_\mathrm{p})}[x_3^3]_e^{e+h_\mathrm{p}} \left| \iint_A w_{,11}|w_{,11}| + 2w_{,11}w_{,22} + w_{,22}|w_{,22}|\,\mathrm{d}x_2\,\mathrm{d}x_1 \right|, \tag{53}$$

where the absolute value operation for the integral assures a positive energy. This formulation allows the calculation of the stored electrical energy independent of the strain polarity within the piezo-wafer.

Using a slender piezoelectric element results in a uniaxial stress field within the element, where only $\sigma_1 \neq 0$. This gives rise to the effective strain energy for a slender piezo element as derived in Ref. [10]

$$U_{\mathrm{eff}} = \frac{1}{2}\frac{d_{31}^2}{\tilde{\varepsilon}_{33}s_{11}} E_\mathrm{p} \left[\frac{x_3^3}{3}\right]_e^{e+h_\mathrm{p}} \left| \iint_A w_{,11}(x_1)|w_{,11}(x_1)|\,\mathrm{d}x_1\,\mathrm{d}x_2 \right|. \tag{54}$$

4. Experimental verification

As a test structure for verification a rectangular shaped aluminium plate measuring (505 mm × 500 mm) is used. For damping enhancement two different kinds of piezoelectric materials can be used: polyvinylidene-fluoride (PVDF) or lead–zirconate–titanate (PZT). PVDF is a very flexible material which can be shaped almost arbitrarily. However, its planar coupling coefficient and Young's modulus are comparatively low. A PZT-element on the other hand is rather brittle. However, its k_p is about 16 times higher, resulting in a loss factor which is 170 times higher. Additionally, it has to be pointed out that the loss factor according to

Table 1
Coordinates of applied PZT-elements [m]

	PZT pair 1	PZT pair 2	PZT pair 3	PZT pair 4	PZT pair 5	PZT pair 6	PZT pair 7	PZT pair 8
x_1	0.100	0.100	0.100	0.100	0.375	0.375	0.375	0.375
x_2	0.343	0.313	0.168	0.138	0.343	0.313	0.168	0.138

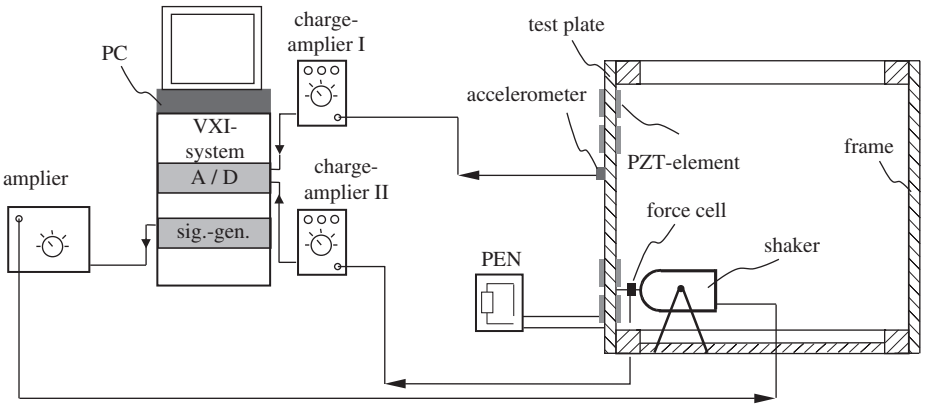

Fig. 6. Setup used to conduct the verification experiments.

Table 2
Eigenfrequencies f_i of plate without and with PZT-elements: experimentally determined (EMA) and numerically calculated (FEM)

	Mode						
	2/1	2/2	1/3	3/1	3/2	4/1	4/2
f_i (Hz), plate w/o PZT (EMA)	161	235	273	288	365	458	550
f_i (Hz), plate w/ PZT (EMA)	150	208	309	283	338	456	530
(FEM)	145	206	295	277	335	464	535

Eq. (45) is proportional to the effective strain energy. This is a function of the Young's modulus, which is also larger for PZT. For this reason PZT-elements are chosen for damping enhancement of the plate. These elements are commercially available with a length of 20–70 mm, a width of 5–25 mm and a thickness of 0.1–1 mm. For bending wavelengths between 190 and 320 mm in the frequency band of interest, elements measuring (70 mm × 25 mm × 1 mm) are chosen to be bonded onto the plate.

For optimal placement of the PZT-elements the following steps have to be considered: (1) identification of the eigenfrequencies and modeshapes within the frequency range of interest; (2) choosing positions for the PZT-elements which are at or close to the maximum of curvature for the modeshape of interest; (3) calculation of the effective strain energy according to Eq. (53) and the resulting loss factor, according to Eq. (45).

For the experimental verification, a total of 16 PZT-elements are bonded on the plate (eight on each side). The center positions are summarized in Table 1, where $(x_1, x_2) = (0, 0)$ is located in one corner of the plate.

The experimental setup is depicted in Fig. 6. As shown, the plate is mounted on a frame structure in such a way that fixed-fixed boundary conditions are obtained. For such boundary conditions the eigenfrequencies and modeshapes for a plate can be calculated analytically, as outlined in Ref. [24]. The plate is excited using a shaker which is driven by a signal generator. In order to identify the plate's modal parameters, acceleration sensors are fixed on the plate, and a force gauge is mounted on the shaker. The PEN is realized by the use of

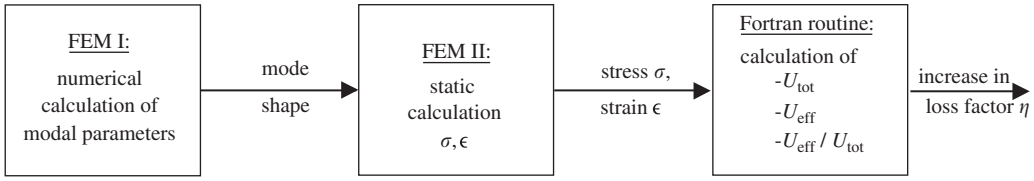

Fig. 7. Flow chart of FE-based calculation.

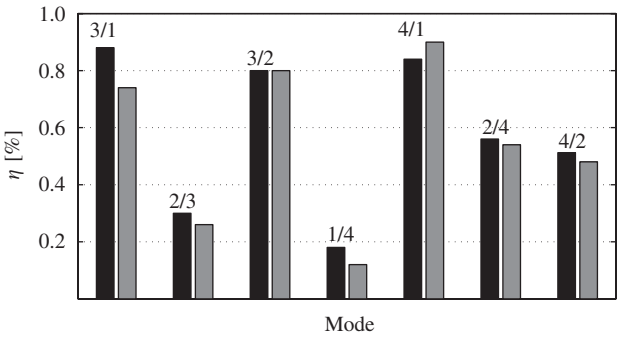

Fig. 8. Increase of loss factor η: FE-based model (black) and experimentally determined (gray).

commercially available resistors. The PEN is tuned in such a way, that the frequency for the maximum loss factor, Eq. (41), coincides with the eigenfrequency of the 3/2-mode. According to this 3/2 designation, there are 3 antinodes in the x_1-direction and 2 antinodes in the x_2-direction. One resistor is connected to every PZT-element to obtain a proper shunt mechanism. Measuring the eigenfrequencies of the plate before and after PZT-elements have been bonded indicates a significant shift of all eigenfrequencies, as can be seen in Table 2. This is due to the added stiffness and inertia caused by the PZT elements. A finite element model of the composite plate is therefore required to accurately predict the strain energy and loss factor.

4.1. Finite-element model of the test plate

For the discretization of the structure shell elements having four nodes per element are used. These elements are isoparametric. Pre-studies showed that a 47×48 grid of elements was fine enough to predict the plate's dynamic response accurately up to 600 Hz. The bonding-layer with a thickness between 80 and 100 μm was not modeled, since its influence is considered to be negligible within the frequency range of interest. The PZT-elements are also modeled using shell elements. Calculation of the resulting loss factor is carried out in three steps: (1) The modal parameters of the plate with PZT-elements are computed using the FE-model (Fig. 7). The resulting eigenfrequencies are compared in Table 2 with the experimentally obtained ones. (2) The resulting displacement field from the modal simulation is assigned as a boundary condition in the FE-model. A static FE simulation yields the stresses σ and stains ε in the plate and the PZT-elements as well as the total strain energy. Simulations are carried out using the software MARC/Mentat© [26]. (3) The resulting nodal values for stress and strain are fed into a FORTRAN-routine, which computes the effective strain energy, according to Eq. (53).

4.2. Comparison of damping enhancement: model and experiment

A direct measurement of the damping enhancement is not possible. Instead the frequency response function for short circuited and shunted PZT-elements is determined. The short circuit case ($R = 0\,\Omega$) yields the inherent damping of the structure, because according to Eq. (39), the PEN yields no damping enhancement. Maximal damping in the frequency range of interest is obtained by shunting each PZT-element with

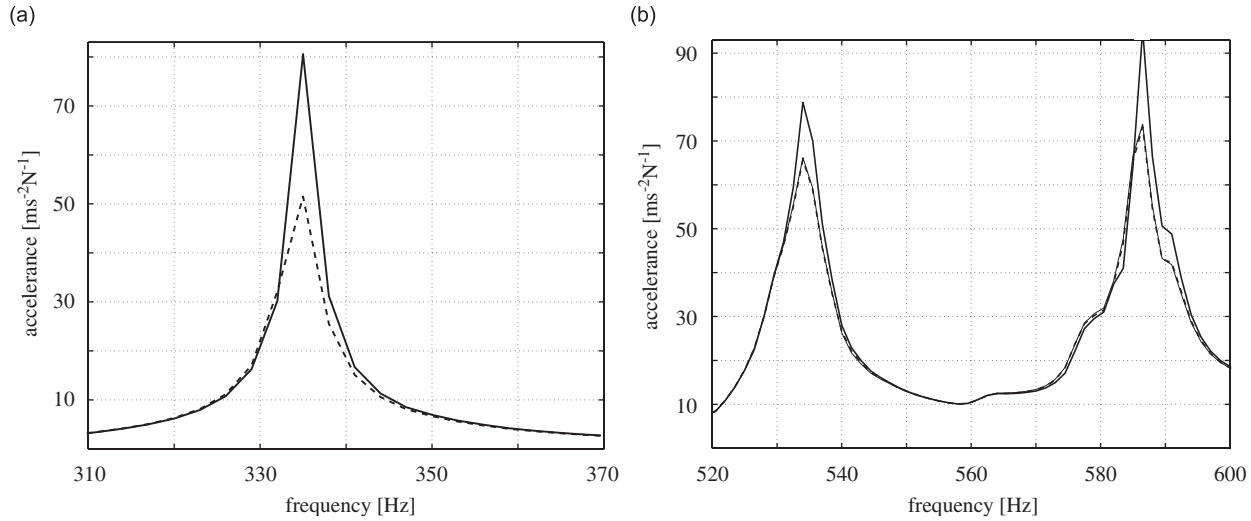

Fig. 9. Experimentally obtained plate accelerance in open loop (—) and shunted (- - -) case: (a) mode 3/2, (b) mode 4/2 and 2/4.

Table 3
Resistance values R used to investigate the effect of damping enhancement

Resistance R (kΩ)	0.012	0.12	0.8	2	4.7	8.2	10	15
Increase of η (%)	0.01	0.07	0.12	0.23	0.52	0.69	0.78	0.84
Resistance R (kΩ)	17	20	25	49	110	1000	–	–
Increase of η (%)	0.82	0.80	0.75	0.56	0.42	0.24	–	–

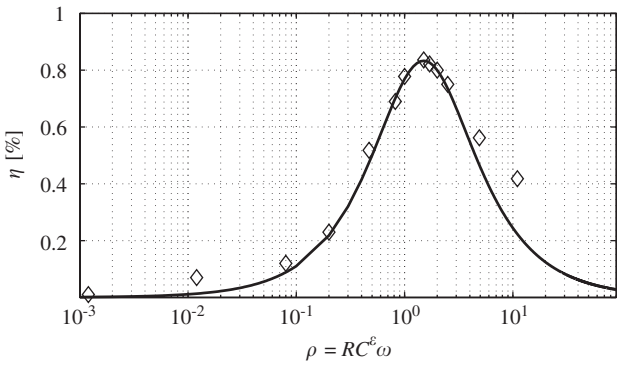

Fig. 10. Dependence of loss factor η on the resistance of the PEN: model-based (—) and experimentally determined (◇).

$R = 15\,\mathrm{k\Omega}$. For a linear system the enhancement in structural damping is given as

$$\Delta\xi = \xi|_{R=15\,\mathrm{k\Omega}} - \xi|_{R=0}. \tag{55}$$

The experimentally determined damping enhancement is depicted in Fig. 8 and is compared to the numerically calculated increase in loss factor for each structural mode. For this comparison the relationship between loss factor η_i and structural damping coefficient ξ_i for each mode i,

$$\eta_i \approx 2\xi_i, \tag{56}$$

in the proximity of a structural resonance is used [27]. The experimentally determined and calculated increase in damping are in very good accordance for all modes.

Additionally, the damping effect is illustrated in the time domain. For this comparison measured accelerances of the open-loop and shunted plate are plotted. Due to the high modal density of the plate under investigation, only some modes are displayed. Fig. 9(a) shows the measured accelerance for mode $3/2$, where the obtained accelerances for mode $4/2$ and $2/4$ are plotted in Fig. 9(b).

4.3. Effect on damping enhancement by the PEN

Finally, the dependency of the loss factor on the dimensionless frequency $\rho = RC^{\mathscr{E}}\,\omega$ is investigated. The resistance R is variable, as listed in Table 3, whereas the parameters $C^{\mathscr{E}}, \omega$ are kept constant. In this experiment all PZT-elements are connected to a PEN. The experimentally determined increase in loss factor is listed in Table 3. The increase in loss factor is computed according to equation (39) and is graphically illustrated in Fig. 10 as a line. Maximal damping for the $3/2$-mode is expected for $R = 15\,\mathrm{k\Omega}$, which is verified by means of this experiment. The damping characteristic for different resistances of the PEN can be described very good by the chosen model of piezo-resistive damping. Merely selecting a resistance much higher than the optimum results in some deviation.

5. Conclusions

Within this paper a model of semi-passive damping enhancement for vibrating two-dimensional structures has been proposed. This damping treatment consists of piezoelectrics in combination with a passive electrical network which dissipates part of the mechanical energy. From a practical point of view the resistive PEN is preferred, since it is easy to realize, inexpensive, and the damping increase for vibrating structures can be very significant. Using basic concepts a new, more general description of this damping measure has been developed. It was illustrated that the models known in literature for one-dimensional structures can be easily extracted out of the more general two-dimensional model. It has been shown that the choice of a proper piezoelectric material—in terms of the coupling coefficient and Young's modulus—and resistance of the PEN is of utmost importance in order to achieve a high efficiency using the proposed damping measure. Furthermore, it has been demonstrated that the loss factor is a nonlinear function of the planar coupling coefficient. Consequently, the existence of a critical coupling coefficient has been proven. Exceeding this critical coupling coefficient does not result in any further increase of loss factor.

For optimal placement of the piezoelectric elements onto the vibrating structure, a general model of the effective strain energy was invented. Compared to already existing approaches in literature this model can also be applied for two-dimensional structures. The optimal placement of piezoceramics which achieves the highest damping, is determined by maximizing the ratio of the effective strain energy to the total strain energy. For this computation, the mode shapes of the structure must be known. Care has to be taken in using analytical formulations of the mode shapes, since the PZT wafers stiffen the structure considerably. A finite-element model provides a more accurate prediction of the strain energy.

Experiments conducted on a plate-like structure verified the models for this type of damping enhancement. Using eight pairs of piezoceramic wafers increased the loss factor of the entire structure by 0.9% for specific structural modes. Finally, it has to be noted that these results were achieved with only a marginal increase in total structural mass, and, the additional amount of damping is almost insensitive to temperature changes within a wide temperature regime.

Acknowledgement

The research presented here was conducted at the Institute A of Mechanics at the University of Stuttgart, Germany.

Support for this research has been provided by the Deutsche Forschungsgemeinschaft (German Science Foundation) under Grant no. Ga 209/26 and the Elisabeth-und-Fridrich-Boysen Stiftung, Germany.

References

[1] R. Forward, Electromechanical transducer-coupled mechanical structure with negative capacitance compensation circuit, US Patent No. 4 158 787, 1979.
[2] R. Edwards, R. Miyakawa, Large structure damping task report. in: Hughes Aircraft Report No. 4132.22/1408, 1980.
[3] N. Hagood, A. von Flotow, Damping of structural vibrations with piezoelectric materials and a passive electrical network, *Journal of Sound and Vibration* 146 (1991) 243–268.
[4] G. Lesieutre, Vibration damping and control using shunted piezoelectric materials, *The Shock and Vibration Digest* 30 (3) (1998) 187–195.
[5] S. Moheimani, A survey of recent innovations in vibration damping and control using shunted piezoelectric transducers, *IEEE Transaction on Control Systems Technology* 11 (4) (2003) 482–494.
[6] M. Ozer, T. Royston, Passively minimizing structural sound radiation using shunted piezoelectric materials, *Journal of the Acoustical Society of America* 1144 (4) (2002) 1934–1946.
[7] J. Tang, K. Wang, Active-passive hybrid piezoelectric networks for vibration control: comparisons and improvements, *Smart Materials and Structures* 10 (2000) 794–806.
[8] C. Park, K. Kabeya, D. Inman, Enhanced piezoelectric shunt design, *Adaptive Structures and Smart Material Systems, Transaction of ASME* 57 (1998) 149–155.
[9] H. Law, P. Rossiter, G. Simon, L. Koss, Characterization of mechanical vibration damping by piezoelectric materials, *Journal of Sound and Vibration* 194 (4) (1996) 489–513.
[10] C. Davis, G. Lesieutre, A modal strain energy approach to the prediction of resistively shunted piezoceramic damping, *Journal of Sound and Vibration* 184 (1) (1995) 129–139.
[11] J. Park, H. Kim, S. Choi, Design and experimental validation of piezoelectric shunt structures using admittance analysis, *Smart Materials and Structures* 15 (4) (2006) 93–103.
[12] M. Tsai, K. Wang, On the structural damping characteristics of active piezoelectric actuators with passive shunt, *Journal of Sound and Vibration* 221 (1999) 1–22.
[13] J. Kim, K. Lee, Broadband transmission noise reduction of smart panels featuring piezoelectric shunt circuits and sound absorbing materials, *Journal of the Acoustical Society of America* 112 (2002) 900–1008.
[14] T. Ikeda, *Fundamentals of Piezoelectricity*, Oxford Science Publications, Oxford, 1990.
[15] H. Linse, *Elektrotechnik für Maschinenbauer*, Teubner-Verlag, Stuttgart, 1992.
[16] O. Fein, L. Gaul, On the application of shunted piezoelectric material to enhance structural damping of a plate, *Journal of Intelligent Material Systems and Structures* 15 (2004) 737–743.
[17] O. Fein, *Ein semi-passives Konzept zur multi-modalen Schwingungsreduktion flächenhafter Strukturen*, Der Andere Verlag, Tönning, 2005.
[18] L. Gaul, O. Fein, Reduction of structural vibrations using piezoelectric material and a passive electrical network, *Proceedings of the 13th International Conference on Adaptive Structures and Technologies*, Potsdam, 2002, pp. 598–606.
[19] O. Fein, Vorrichtung zur Einstellung der Dämpfung einer schwingenden Maschinenverkleidung, *German Gebrauchsmuster* 20 2004 008 460.0, 2004.
[20] K. Ruschmayer, *Piezokeramik*, Expert-Verlag, Renningen-Malmsheim, 1995.
[21] A. Joshi, *Matrices and Tensors in Physics*, Wiley, New York, 1995.
[22] Piezoceramic Materials, internet version, http://www.piceramic.de, PI Ceramic, 11.3.2002.
[23] Piezo film sensors, technical manual, internet version, http://www.msiusa.com, Measurement Specialities, 15.6.2002.
[24] C. Wang, *Applied Elasticity*, McGraw-Hill Company, New York, 1953.
[25] P. Dobrinski, G. Krakau, A. Vogel, *Physik für Ingenieure*, eighth ed., Teubner-Verlag, Stuttgart, 1993.
[26] MARC Volume C: program input, online documentation version K7, 1997.
[27] N. Maia, J. Silva, J. He, N. Lieven, R. Lin, G. Skingle, W. To, A. Urugueira, *Theoretical and Experimental Modal Analysis*, Research Studies Press, Baldock, 1997.